How to use the Classical and Quantum Geometric Tensor and its curvature to describe quantum phase transitions

D. Gutiérrez-Ruiz, D. Gonzalez, J. G. Hirsch, J. D. Vergara

Instituto de Ciencias Nucleares, UNAM

J. Chávez-Carlos

Instituto de Ciencias Físicas, UNAM

Ergodicity and chaos in many-body systems, February 7, 2021.

Contents

- Geometry in the parameter space
- Consider a quantum system whose Hamiltonian
- $\hat{H}(x)$depends smoothly on a set of m real adiabatic parameters denoted by $x = \{x^i\}$.
- For an orthonormal eigenvector $|n(x)\rangle$ of the system with non-degenerate eigenvalues the quantum geometric tensor (QGT)

$$Q_{ij}^{(n)} := \langle \partial_i n | \partial_j n \rangle - \langle \partial_i n | n \rangle \langle n | \partial_j n \rangle,$$

- The (symmetric) real part of the QGT yields the Quantum Metric Tensor QMT $g_{ij}^{(n)} = \mathrm{Re}\, Q_{ij}^{(n)},$
- The (antisymmetric) imaginary part of the QGT encodes the Berry curvature $F_{ij}^{(n)} = -2\,\mathrm{Im}\, Q_{ij}^{(n)},$

Inserting the identity operator $\mathbb{I} = \sum_m |m\rangle\langle m|$,

$$\langle m|\partial_i n\rangle = \frac{\langle m|\partial_i \hat{H}|n\rangle}{E_n - E_m} \qquad \text{for} \qquad m \neq n,$$

we rewrite the QGT as

$$Q_{ij}^{(n)} = \sum_{m\neq n} \frac{\langle n|\partial_i \hat{H}|m\rangle\langle m|\partial_j \hat{H}|n\rangle}{(E_m - E_n)^2}.$$

using the path integral formalism, it is possible to rewrite the QGT as [JHEP 2017]

$$Q_{AB}^{(m)} = -\int_{-\infty}^{0} d\tau_1 \int_{0}^{\infty} d\tau_2 \left[\langle m|\, \mathcal{O}_A(\tau_1)\mathcal{O}_B(\tau_2)\,|m\rangle - \langle m|\, \mathcal{O}_A(\tau_1)\,|m\rangle\,\langle m|\, \mathcal{O}_B(\tau_2)\,|m\rangle\right].$$

where the deformation functions are defined as

$$\hat{\mathcal{O}}_A = \frac{\partial \hat{H}}{\partial x^A}$$

$H = H_0 + \delta H$

The real part can be written as

$$\mathbf{Re}\,\mathrm{G}_{ab}=\int_{-\infty}^{0}\mathrm{d}\tau_1\int_{0}^{\infty}\mathrm{d}\tau_2\left(\frac{1}{2}\left(\langle\mathcal{O}_a(\tau_1)\mathcal{O}_b(\tau_2)\rangle+\langle\mathcal{O}_b(\tau_1)\mathcal{O}_a(\tau_2)\rangle\right)-\langle\mathcal{O}_a(\tau_1)\rangle\langle\mathcal{O}_b(\tau_2)\rangle\right)=$$

$$=\int_{-\infty}^{0}d\tau_1\int_{0}^{\infty}d\tau_2\left(\frac{1}{2}\langle\{\mathcal{O}_a(\tau_1),\mathcal{O}_b(\tau_2)\}\rangle-\langle\mathcal{O}_a(\tau_1)\rangle\langle\mathcal{O}_b(\tau_2)\rangle\right),$$

whereas the imaginary part takes the form

$$\mathbf{Im}\,\mathrm{G}_{ab}=\frac{1}{2\mathrm{i}}\int_{-\infty}^{0}\mathrm{d}\tau_1\int_{0}^{\infty}\mathrm{d}\tau_2\left(\langle\mathcal{O}_a(\tau_1)\mathcal{O}_b(\tau_2)\rangle-\langle\mathcal{O}_b(\tau_1)\mathcal{O}_a(\tau_2)\rangle\right)=\frac{1}{2\mathrm{i}}\int_{-\infty}^{0}\mathrm{d}\tau_1\int_{0}^{\infty}\mathrm{d}\tau_2\,\langle[\mathcal{O}_a(\tau_1),\mathcal{O}_b(\tau_2)]\rangle,$$

The real part corresponds to the Quantum Information Metric

$$g_{ab}=\int_{-\infty}^{0}d\tau_1\int_{0}^{\infty}d\tau_2\left(\frac{1}{2}\langle\{\mathcal{O}_a(\tau_1),\mathcal{O}_b(\tau_2)\}\rangle-\langle\mathcal{O}_a(\tau_1)\rangle\langle\mathcal{O}_b(\tau_2)\rangle\right),\quad(3)$$

Classical analogue of the Quantum Metric and Berry Curvature [Ann.Physik 2019]

$$g_{ab}(x) = -\int_{-\infty}^{0} dt_1 \int_{0}^{\infty} dt_2 \Big(\langle \mathcal{O}_a(t_1)\mathcal{O}_b(t_2)\rangle_{\mathrm{cl}} - \langle \mathcal{O}_a(t_1)\rangle_{\mathrm{cl}} \langle \mathcal{O}_b(t_2)\rangle_{\mathrm{cl}} \Big),$$

where the $\mathcal{O}_a(t)$ are the classical deformation functions, that can be written in terms of the initial conditions (q_0, p_0) and time, and subsequently, in terms of the initial action-angle variables (ϕ_0, I) and here the classical averages corresponds to

$$\langle f \rangle_{\mathrm{cl}} = \frac{1}{(2\pi)^n} \int_0^{2\pi} \mathrm{d}^n\phi_0 \, f(\phi_0, I, t; x)$$

$$I = \oint p \, dq$$

Now that we have endowed our parameter space with a metric structure, we can construct a quantity that contains all the local information of the curvature of our manifold in the case of two dimensions: the scalar curvature, also known as the Ricci scalar.

The scalar curvature in two dimensions can be computed as

$$R = \frac{1}{\sqrt{|g|}}(\mathscr{A} + \mathscr{B})$$

with $g = \det[g_{ab}]$, and

$$\mathscr{A} := \partial_1 \left(\frac{g_{12}}{g_{11}\sqrt{|g|}} \partial_2 g_{11} - \frac{1}{\sqrt{|g|}} \partial_1 g_{22} \right),$$

$$\mathscr{B} := \partial_2 \left(\frac{2}{\sqrt{|g|}} \partial_1 g_{12} - \frac{1}{\sqrt{|g|}} \partial_2 g_{11} - \frac{g_{12}}{g_{11}\sqrt{|g|}} \partial_1 g_{11} \right).$$

THE DICKE MODEL

The Hamiltonian of the Dicke model is

$$\hat{H} = \omega_0 \hat{J}_z + \omega \hat{a}^\dagger \hat{a} + \frac{\lambda}{\sqrt{N}}(\hat{a}^\dagger + \hat{a})(\hat{J}_+ + \hat{J}_-),$$

Analysis in the thermodynamic limit

Normal phase

The Holstein-Primakoff transformation leads to the effective Hamiltonian

$$\hat{H}_n = -j\omega_0 - \frac{(\omega + \omega_0)}{2} + \frac{1}{2}\left(\hat{p}_1^2 + \hat{p}_2^2 + \omega^2 \hat{q}_1^2 + \omega_0^2 \hat{q}_2^2 + 4\lambda\sqrt{\omega\omega_0}\, \hat{q}_1 \hat{q}_2 \right).$$

that in normal coordinates has the form

$$\hat{H}_n = -j\omega_0 - \frac{(\omega + \omega_0)}{2} + \frac{1}{2}\left(\hat{P}_1^2 + \hat{P}_2^2 + \varepsilon_{1n}^2 \hat{Q}_1^2 + \varepsilon_{2n}^2 \hat{Q}_2^2 \right),$$

where the two normal frequencies are

$$\varepsilon_{1n}^2 = \frac{1}{2}\left[\omega^2 + \omega_0^2 - \sqrt{(\omega^2 - \omega_0^2)^2 + 16\lambda^2\omega\omega_0}\right],$$

$$\varepsilon_{2n}^2 = \frac{1}{2}\left[\omega^2 + \omega_0^2 + \sqrt{(\omega^2 - \omega_0^2)^2 + 16\lambda^2\omega\omega_0}\right].$$

Superradiant phase

Effective Hamiltonian in normal coordinates

$$\hat{H}_s = -j\left(\frac{2\lambda^2}{\omega} + \frac{\omega_0^2\omega}{8\lambda^2}\right) - \frac{4\lambda^2 + \omega^2}{2\omega} + \frac{1}{2}\left(\hat{P}_1^2 + \hat{P}_2^2 + \varepsilon_{1s}^2\hat{Q}_1^2 + \varepsilon_{2s}^2\hat{Q}_2^2\right),$$

The two resulting normal frequencies are

$$\varepsilon_{1s}^2 = \frac{1}{2}\left[\frac{16\lambda^4 + \omega^4}{\omega^2} - \sqrt{\left(\frac{16\lambda^4 - \omega^4}{\omega^2}\right)^2 + 4\omega^2\omega_0^2}\right],$$

$$\varepsilon_{2s}^2 = \frac{1}{2}\left[\frac{16\lambda^4 + \omega^4}{\omega^2} + \sqrt{\left(\frac{16\lambda^4 - \omega^4}{\omega^2}\right)^2 + 4\omega^2\omega_0^2}\right].$$

Considering a two dimensional parameter manifold with coordinates $x = \{x^i\} = (\omega, \lambda), i = 1,2$ and deformation functions (or operators in the quantum case) in the **normal phase**

$$\mathcal{O}_{1n} = \frac{\partial H_n}{\partial \omega} = \omega q_1^2 + \lambda \sqrt{\frac{\omega_0}{\omega}}\, q_1 q_2,$$

$$\mathcal{O}_{2n} = \frac{\partial H_n}{\partial \lambda} = 2\sqrt{\omega \omega_0}\, q_1 q_2,$$

We obtain the classical metric for the normal phase,

$$g_{ij\ cl} = \frac{\partial_i \varepsilon_{1n} \partial_j \varepsilon_{1n}}{8\varepsilon_{1n}^2} I_1^2 + \frac{\partial_i \varepsilon_{2n} \partial_j \varepsilon_{2n}}{8\varepsilon_{2n}^2} I_2^2 + \partial_i \alpha_n \partial_j \alpha_n \left(\frac{\varepsilon_{1n}}{\varepsilon_{2n}} + \frac{\varepsilon_{2n}}{\varepsilon_{1n}} \right) I_1 I_2 \,.$$

and the quantum metric for the ground state is given by

$$g_{ij}^{(0)} = \frac{\partial_i \varepsilon_{1n} \partial_j \varepsilon_{1n}}{8\varepsilon_{1n}^2} + \frac{\partial_i \varepsilon_{2n} \partial_j \varepsilon_{2n}}{8\varepsilon_{2n}^2} + \partial_i \alpha_n \partial_j \alpha_n \left[\frac{1}{4} \left(\frac{\varepsilon_{1n}}{\varepsilon_{2n}} + \frac{\varepsilon_{2n}}{\varepsilon_{1n}} \right) - \frac{1}{2} \right].$$

Superradiant phase

The deformation functions are now

$$\mathcal{O}_{1s} = \frac{\partial H_s}{\partial \omega} = \omega q_1^2 - \frac{16\lambda^4}{\omega^3} q_2^2 + \omega_0 q_1 q_2, \qquad \mathcal{O}_{2s} = \frac{\partial H_s}{\partial \lambda} = \frac{32\lambda^3}{\omega^2} q_2^2 .$$

and the classical and quantum metrics are

$$g_{ij} = \frac{\partial_i \varepsilon_{1s} \partial_j \varepsilon_{1s}}{8\varepsilon_{1s}^2} I_1^2 + \frac{\partial_i \varepsilon_{2s} \partial_j \varepsilon_{2s}}{8\varepsilon_{2s}^2} I_2^2 + \partial_i \alpha_s \partial_j \alpha_s \left(\frac{\varepsilon_{1s}}{\varepsilon_{2s}} + \frac{\varepsilon_{2s}}{\varepsilon_{1s}} \right) I_1 I_2,$$

$$g_{ij}^{(0)} = \frac{\partial_i \varepsilon_{1s} \partial_j \varepsilon_{1s}}{8\varepsilon_{1s}^2} + \frac{\partial_i \varepsilon_{2s} \partial_j \varepsilon_{2s}}{8\varepsilon_{2s}^2} + \partial_i \alpha_s \partial_j \alpha_s \left[\frac{1}{4} \left(\frac{\varepsilon_{1s}}{\varepsilon_{2s}} + \frac{\varepsilon_{2s}}{\varepsilon_{1s}} \right) - \frac{1}{2} \right],$$

Notice that these metrics have the same form as the previous ones. However, they are quite different in the sense that they are written for two different frequencies.

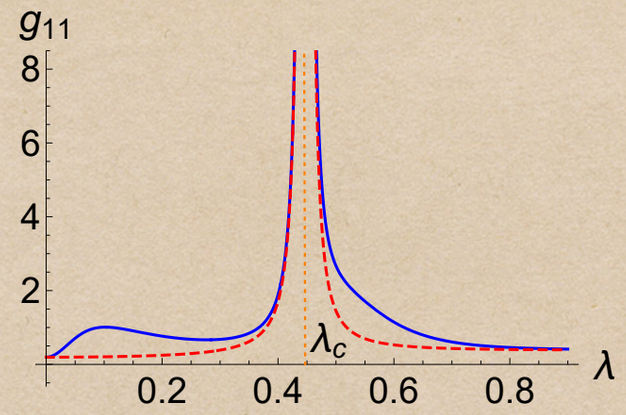

(a)

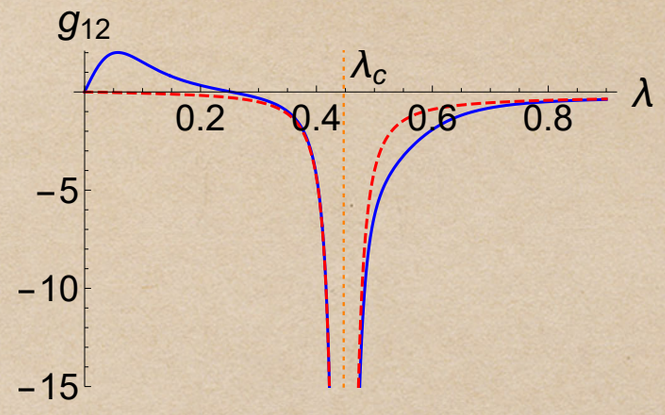

(b)

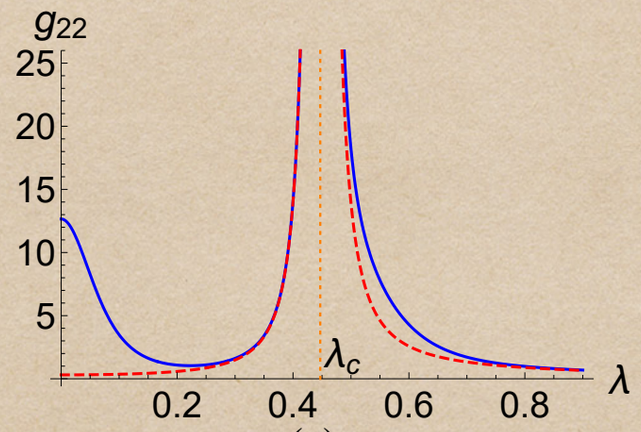

(c)

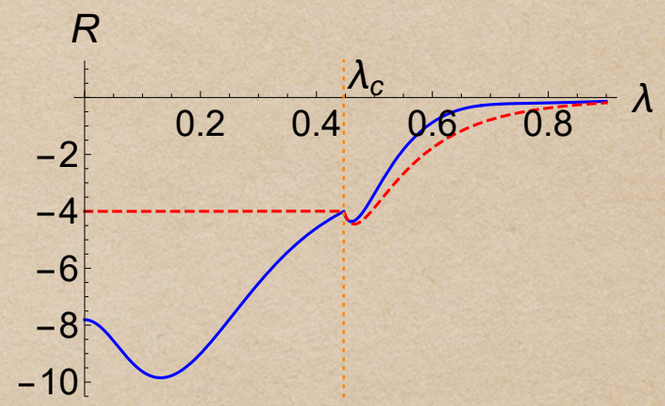

(d)

Metric components and scalar curvature of the classical metric (solid blue) and the quantum metric (dashed red) as a function of when $\omega_0 = 1$ and $\omega = 0.8$. All the components show a divergence at the phase transition (dotted orange) with critical coupling $\lambda_c = 0.447$, whereas the scalar curvature does not.

Metrics under resonance $\omega = \omega_0$

$$g_{12n} = g^{(0)}_{12n} = \frac{\lambda(4\lambda^2 - 3\omega^2)}{8\omega(\omega^2 - 4\lambda^2)^2}, \quad g_{22n} = g^{(0)}_{22n} = \frac{4\lambda^2 + \omega^2}{4(\omega^2 - 4\lambda^2)^2}.$$

$$g_{11n} = \frac{16\lambda^4\omega^3 - 8\lambda^2\omega^5 + \omega^7 + \lambda^2\sqrt{\omega^2 - 4\lambda^2}(8\lambda^4 - 6\lambda^2\omega^2 + 2\omega^4)}{32\lambda^2\omega^2\left(\omega^2 - 4\lambda^2\right)^{5/2}},$$

$$g^{(0)}_{11n} = \frac{-16\lambda^6 + 48\lambda^4\omega^2 - 23\lambda^2\omega^4 + 3\omega^6 - \omega\sqrt{\omega^2 - 4\lambda^2}(4\lambda^4 - 3\lambda^2\omega^2 + \omega^4)}{16\omega^2(\omega^2 - 4\lambda^2)^{5/2}\left(\omega + \sqrt{\omega^2 - 4\lambda^2}\right)}.$$

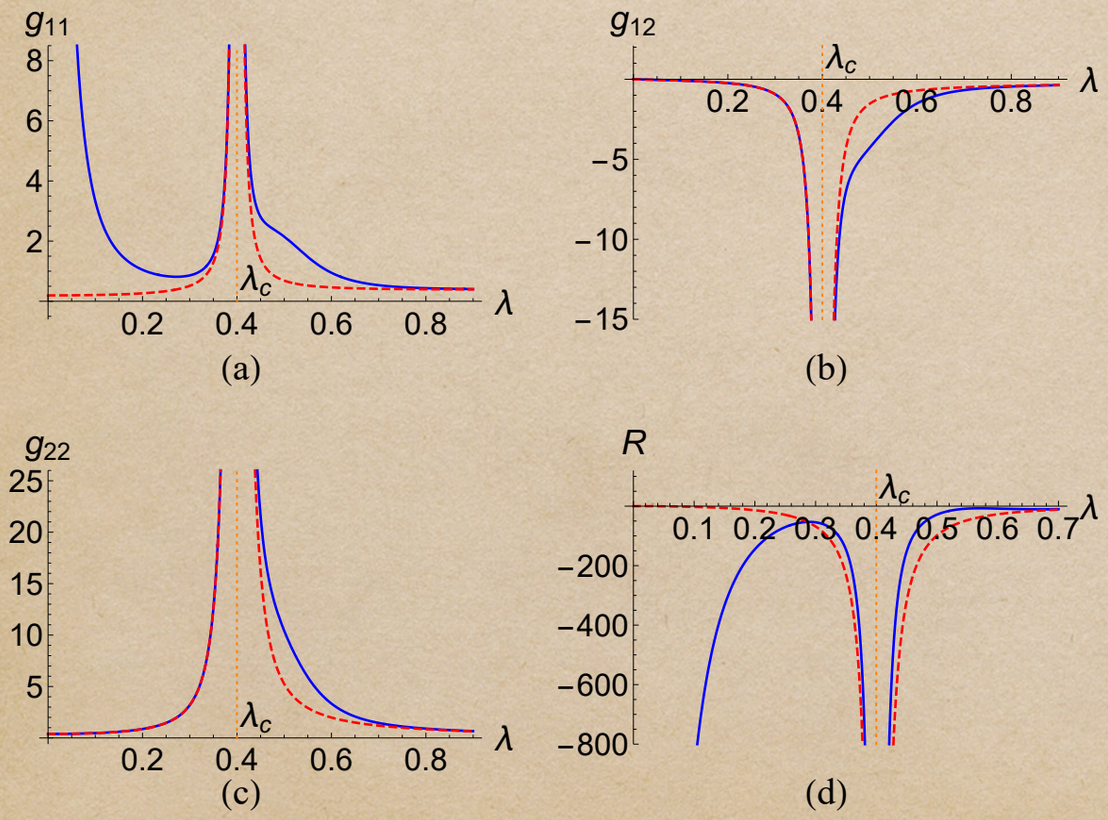

Metric components and scalar curvature of the classical metric (solid blue) and the quantum metric (dashed red) for the resonant case as a function of λ when $\omega_0 = 0.8$. All of them show a divergence at the phase transition (dotted orange) with critical coupling $\lambda_c = 0.4$.

THE LIPKIN-MESHKOV-GLICK MODEL

Hamiltonian

$$\hat{H} = -2h\hat{J}_z - \frac{1}{j}\left(\hat{J}_x^2 + \gamma\hat{J}_y^2\right),$$

Classical Hamiltonian

$$H_{cl} = -2hj + h(P^2+Q^2) - (\gamma P^2+Q^2)\left(1 - \frac{P^2+Q^2}{4j}\right).$$

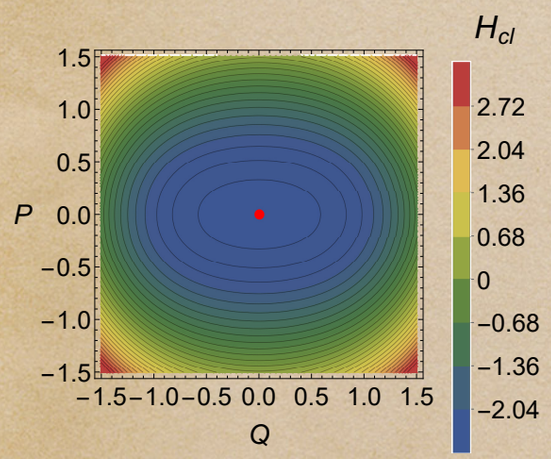

(a)

Symmetric Phase

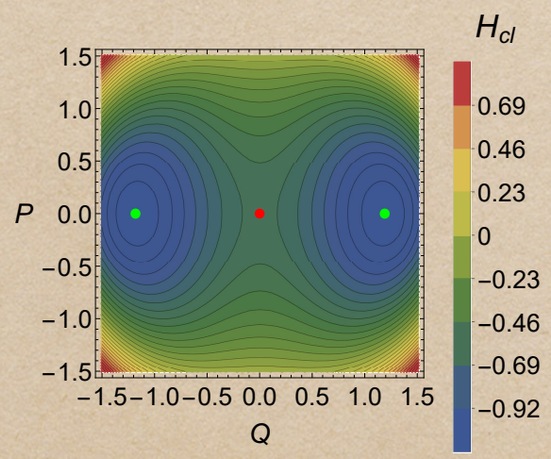

(b)

Broken Phase

Metrics for the symmetric phase under the analytic approximation

$$g_{11} = \frac{I^2}{32}\left[\frac{1-\gamma}{(h-1)(h-\gamma)}\right]^2 = g_{11}^{(0)}(I^2=1)$$

$$g_{12} = \frac{I^2(1-\gamma)}{32(h-1)(h-\gamma)^2} = g_{12}^{(0)}(I^2=1)$$

$$g_{22} = \frac{I^2}{32(h-\gamma)^2} = g_{22}^{(0)}(I^2=1)\,. \qquad \det(g_{ij}) = 0$$

Metrics for the broken phase under the analytic approximation

$$g_{11} = \frac{jI}{\sqrt{(1-h^2)(1-\gamma)}} + \frac{I^2}{32}\left[\frac{h(h^2-\gamma)}{(1-h^2)(1-\gamma)}\right]^2,$$

$$g_{12} = \frac{I^2 h\left(h^2-\gamma\right)}{32\left(1-h^2\right)(1-\gamma)^2},$$

$$g_{22} = \frac{I^2}{32(1-\gamma)^2}\,.$$

with determinant

$$\det g = \frac{I^3}{32\sqrt{(1-h^2)(1-\gamma)^5}},$$

and curvature

$$R = -4 + \frac{7h^4 - (9\gamma - 2)h^2 - 4(1-\gamma)}{j\sqrt{(1-h^2)(1-\gamma)^3}}.$$

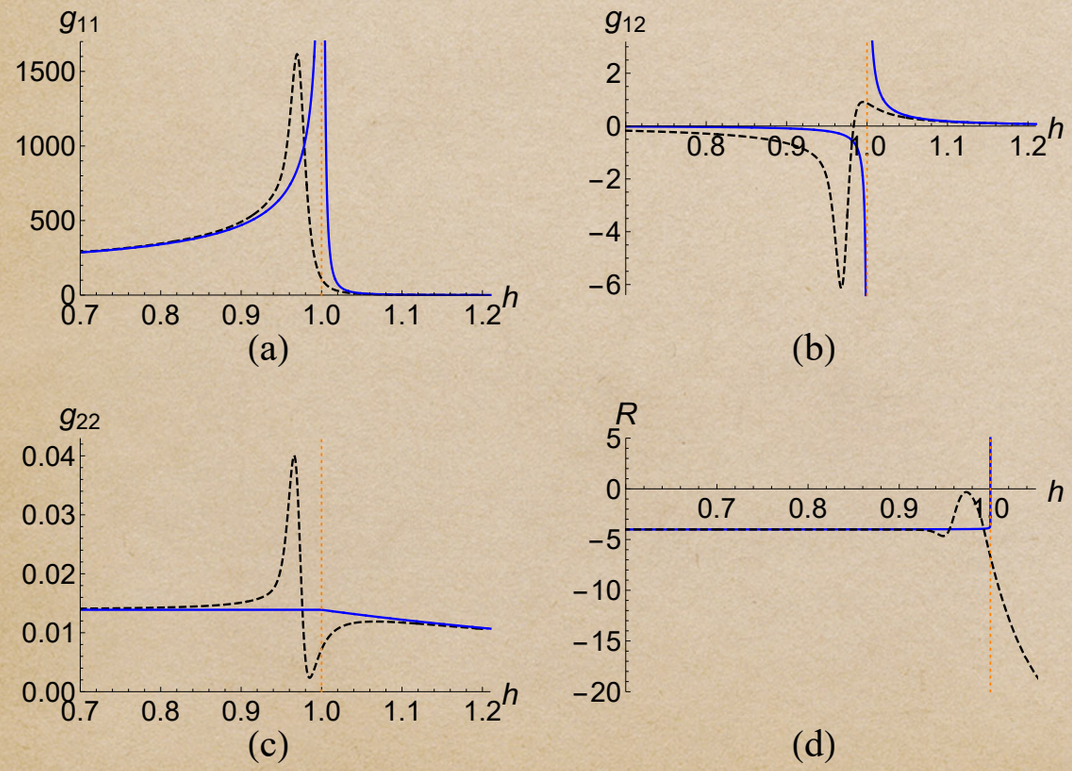

Metric components and scalar curvature of the classical (or quantum) metric in the thermodynamic limit (solid blue) and the exact QMT for $j = 500$ (dashed black)

Numerical analysis for finite j

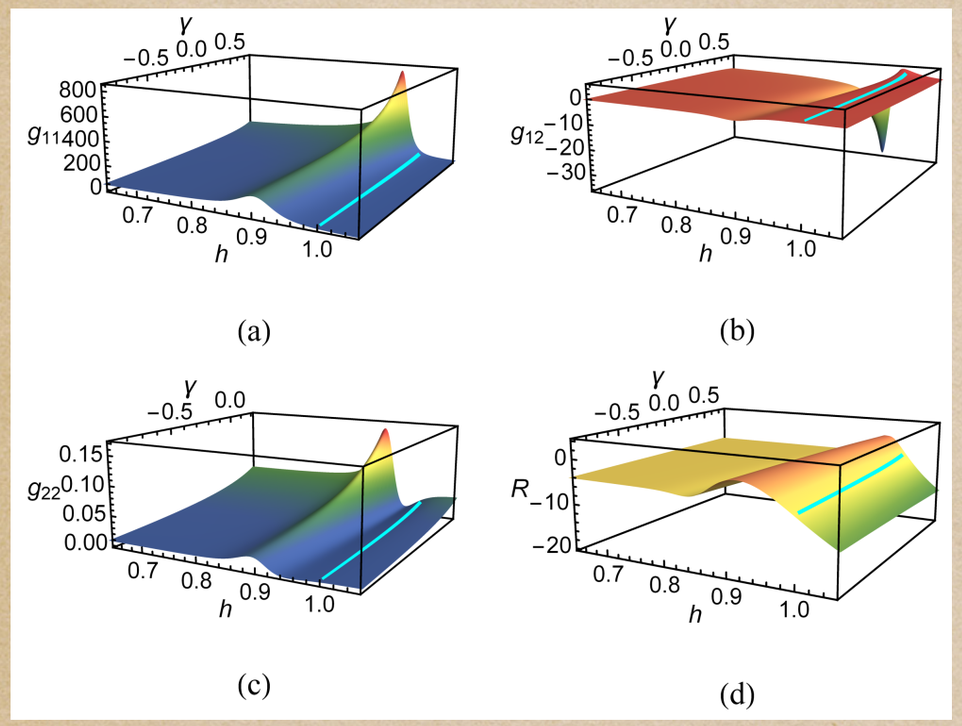

FIG. 4. Metric components and scalar curvature for $j = 100$. The plots clearly show the presence of the QPT precursors. The critical line $h = 1$ is shown in cyan.

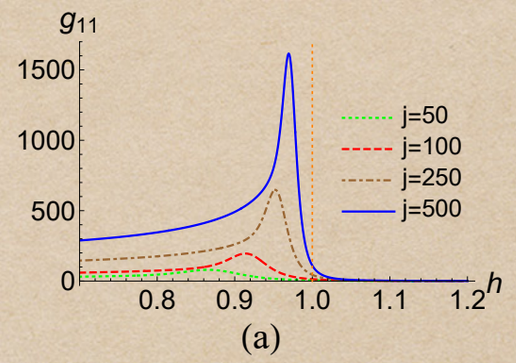

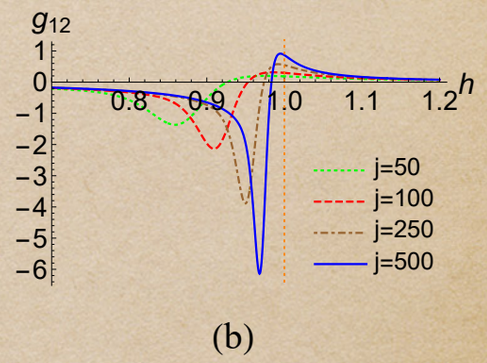

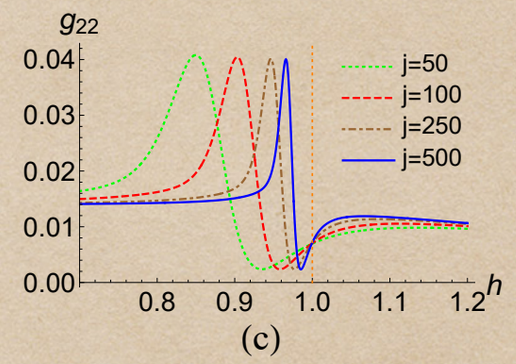

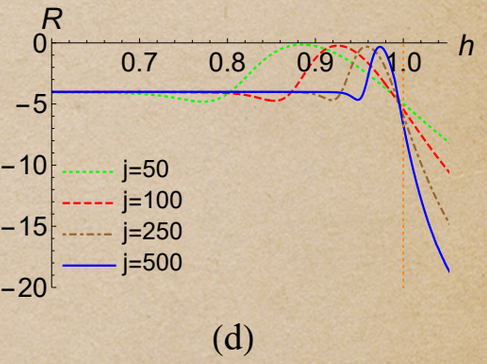

Other version of the Lipkin-Meshkov-Glick model

We shall consider the following Hamiltonian

$$\hat{H}_{\mathrm{LMG}} = \Omega \hat{J}_z + \Omega_x \hat{J}_x + \frac{\xi_y}{j} \hat{J}_y^2,$$

Using a projection on Bloch coherent sates we get

$$h_{\mathrm{LMG}} = \langle z | \hat{H}_{\mathrm{LMG}} | z \rangle / j = -\Omega \cos\theta + \Omega_x \sin\theta \cos\phi + \xi_y \sin^2\theta \sin^2\phi \,.$$

Notice that Hamiltonian is invariant under the interchange $\phi \leftrightarrow -\phi$. Using the canonical variables

$Q = \sqrt{2(1-\cos\theta)}\cos\phi, \quad P = -\sqrt{2(1-\cos\theta)}\sin\phi \,.$

The hamiltonian reads

$$h_{\mathrm{LMG}}(Q,P) = \frac{\Omega}{2}\left(Q^2+P^2\right) - \Omega + \Omega_x Q\sqrt{1-\frac{Q^2+P^2}{4}} + \xi_y P^2\left(1-\frac{Q^2+P^2}{4}\right).$$

This system has four critical points two stable and two inestable.

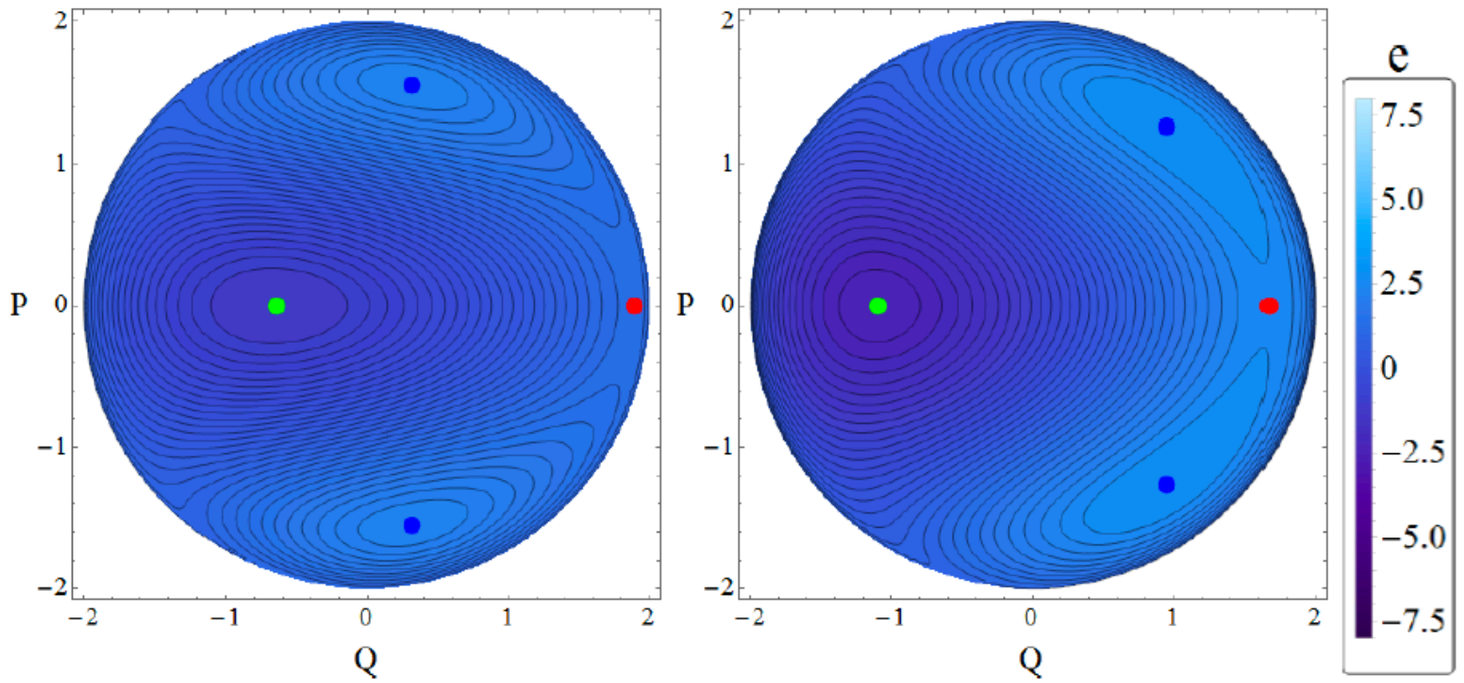

FIG. 5. Energy surfaces for different values of the parameters Ω, with $\Omega_{xc} = \sqrt{4\xi_y^2 - 1}$ with $\xi_y = 2$. Green points are stable center points $\mathbf{x}_2$, the blue ones are unstable center points: $\mathbf{x}_4$ and $\mathbf{x'}_4$ in (a) and (b), and in (c) and (d), and the red point is the critical point with positive Lyapunov exponent $\mathbf{x}_1$, only present in (a) and (b).

GEOMETRY OF THE PARAMETER SPACE OF THE LMG MODEL

a) Ground State

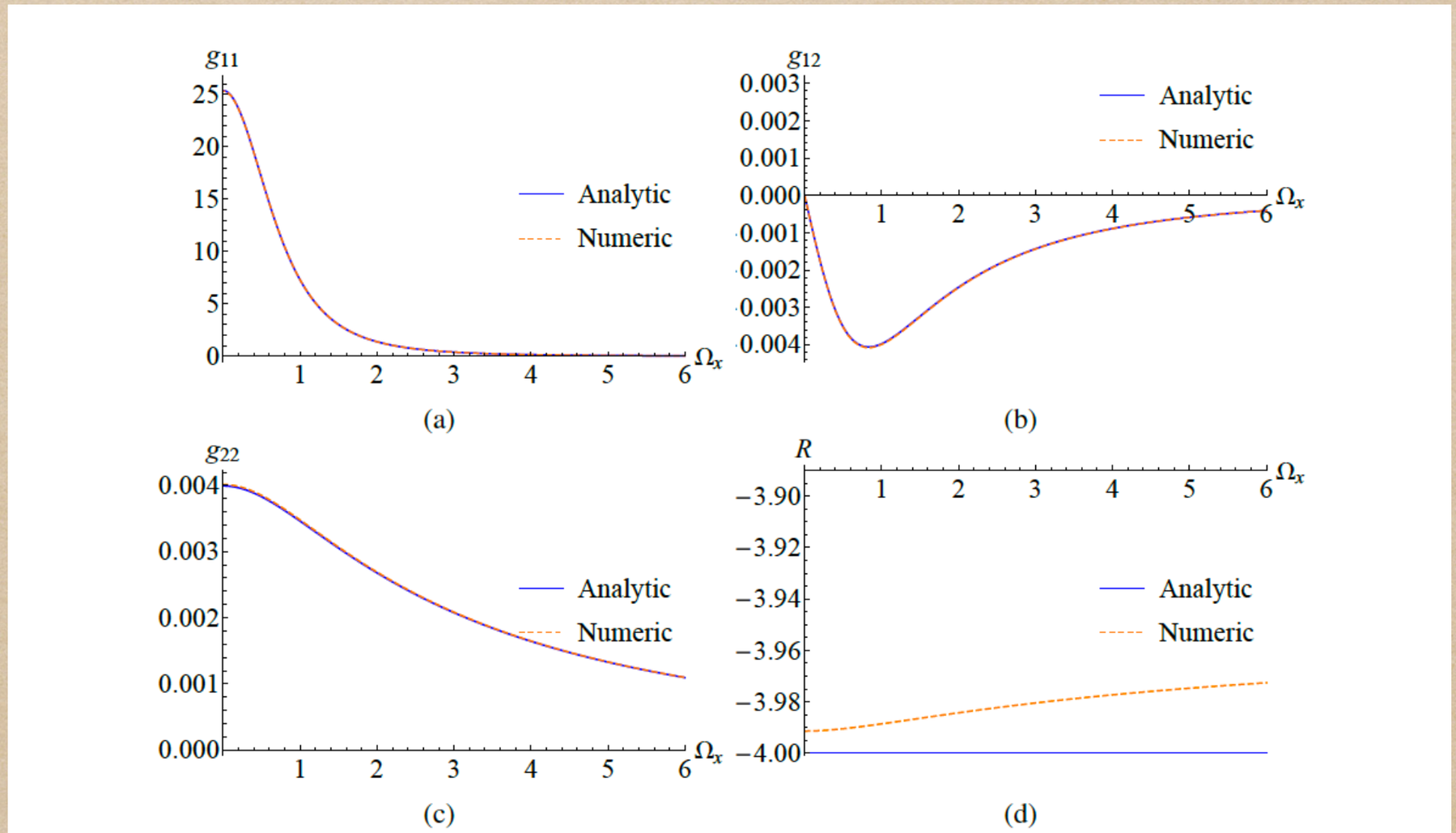

FIG. 7. QMT components and its scalar curvature for the ground state when $j = 120$ and $\xi_y = 2.3$.

B. Highest energy state

Symmetric phase (analytic approximation)

$$g_{11} = \frac{j}{2\left(\Omega_x^2+1\right)^{7/4}\sqrt{\sqrt{\Omega_x^2+1}-2\xi_y}} + \frac{\xi_y^2\Omega_x^2}{8\left(\Omega_x^2+1\right)^2\left(\sqrt{\Omega_x^2+1}-2\xi_y\right)^2},$$

$$g_{12} = -\frac{\xi_y\Omega_x}{8\left(\Omega_x^2+1\right)\left(\sqrt{\Omega_x^2+1}-2\xi_y\right)^2}, \quad g_{22} = \frac{1}{8\left(\sqrt{\Omega_x^2+1}-2\xi_y\right)^2}$$

$$R = -4$$

Broken symmetry phase

Hamiltonian in the analytic approximation

$$\hat{H} \simeq j\frac{4\xi_y^2+\Omega_x^2+1}{4\xi_y} - \frac{\xi_y\left(4\xi_y^2-\Omega_x^2-1\right)}{4\xi_y^2-1}\hat{P}^2 + \frac{\Omega_x\sqrt{4\xi_y^2-\Omega_x^2-1}}{2\left(4\xi_y^2-1\right)}\left(\hat{Q}\hat{P}+\hat{P}\hat{Q}\right) - \frac{16\xi_y^4-8\xi_y^2+\Omega_x^2+1}{4\xi_y\left(4\xi_y^2-1\right)}\hat{Q}^2 .$$

We get a Berry curvature given by

$$F_{12} = -\frac{2j+1}{4\xi_y^2\sqrt{4\xi_y^2-\Omega_x^2-1}} + \frac{16\xi_y^2-\Omega_x^2+1}{16\xi_y^3\left(4\xi_y^2-\Omega_x^2-1\right)} .$$

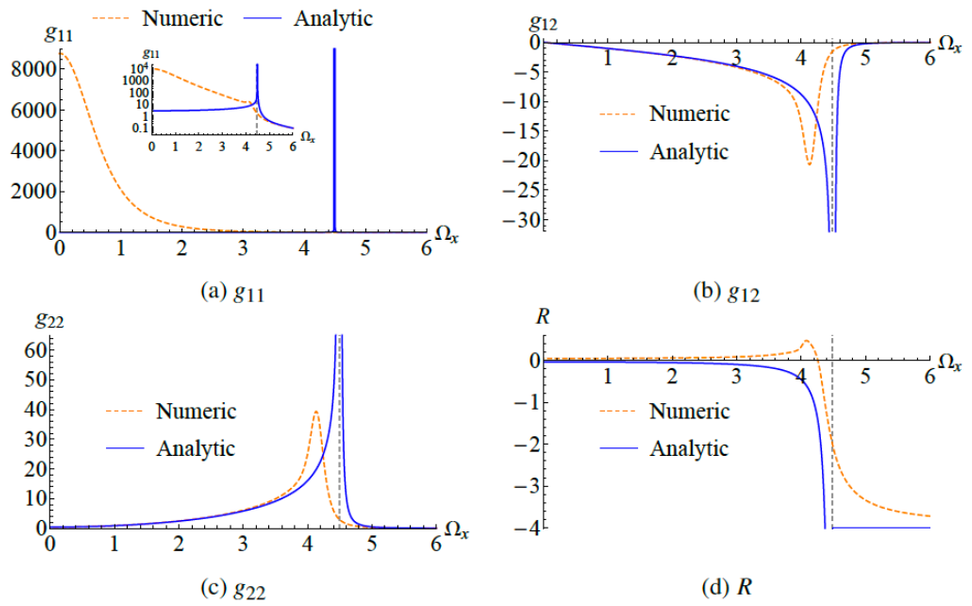

(a) g_{11} (b) g_{12} (c) g_{22} (d) R

FIG. 9. Comparison of the numeric QMT components and the scalar curvature with the analytic results for $\xi_y = 2.3$ and $j = 96$ for the highest energy state. The inset shows the g_{11} component in logarithmic scale. The agreement is excellent except near to the QPT (dashed gray). Notice in the plots of g_{11} the difference between the analytical and numerical curves as $\Omega_x \to 0$.

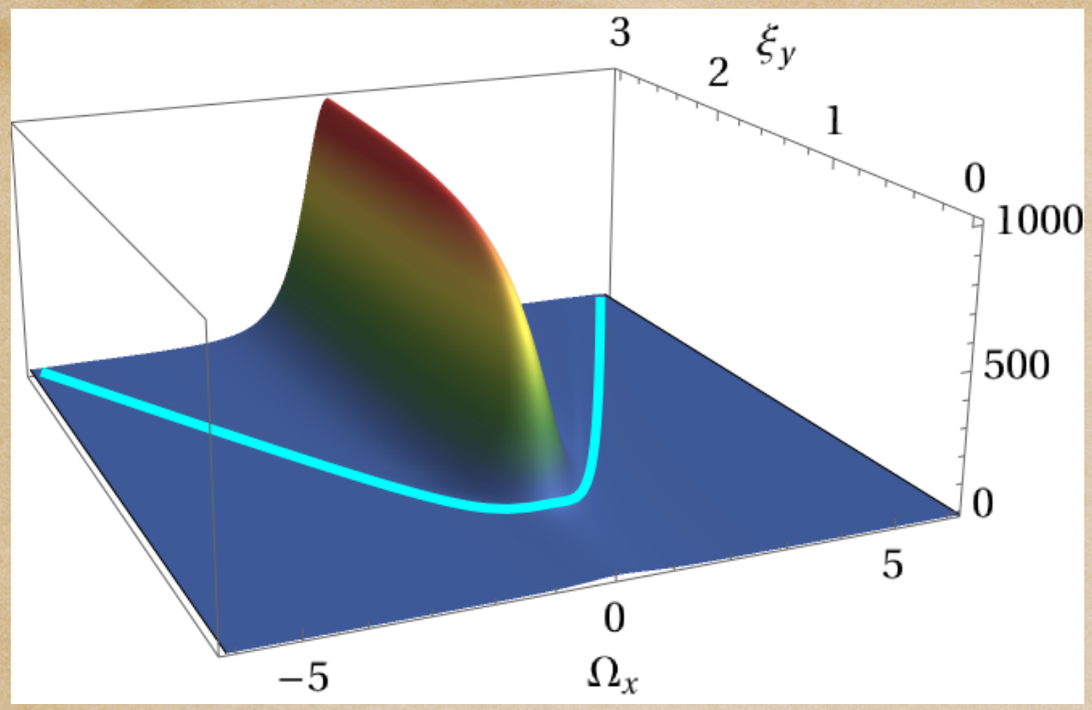
3
2
1
0
ξ_y
1000
500
0
5
0
−5
Ω_x

g_{11}

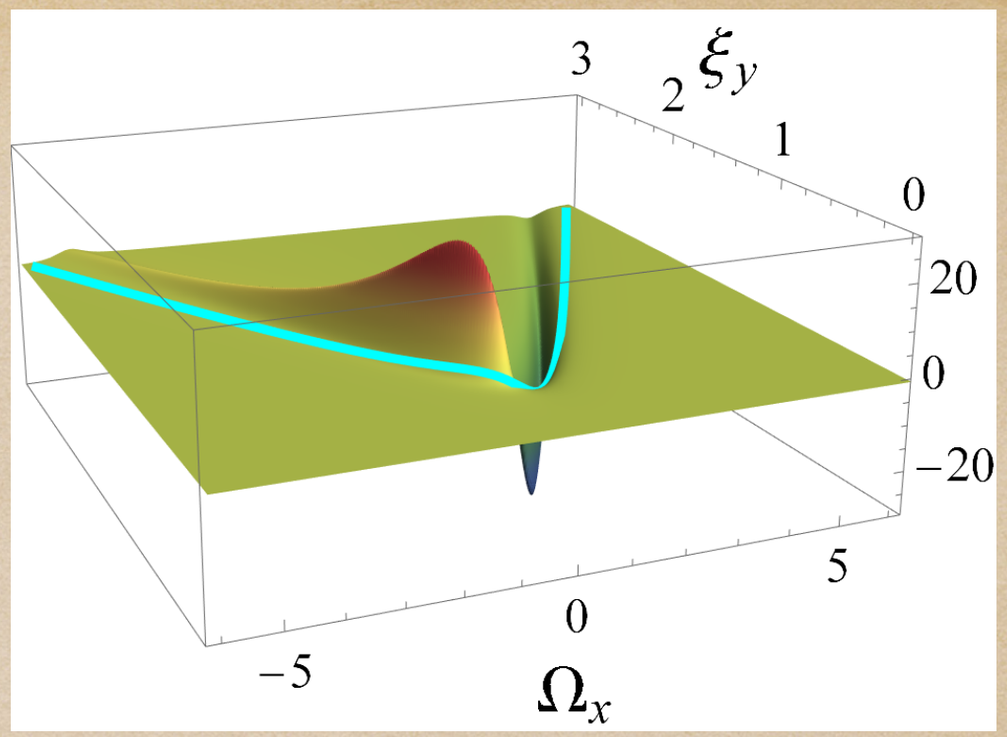
3
2
1
0
ξ_y
20
0
−20
5
0
−5
Ω_x

g_{12}

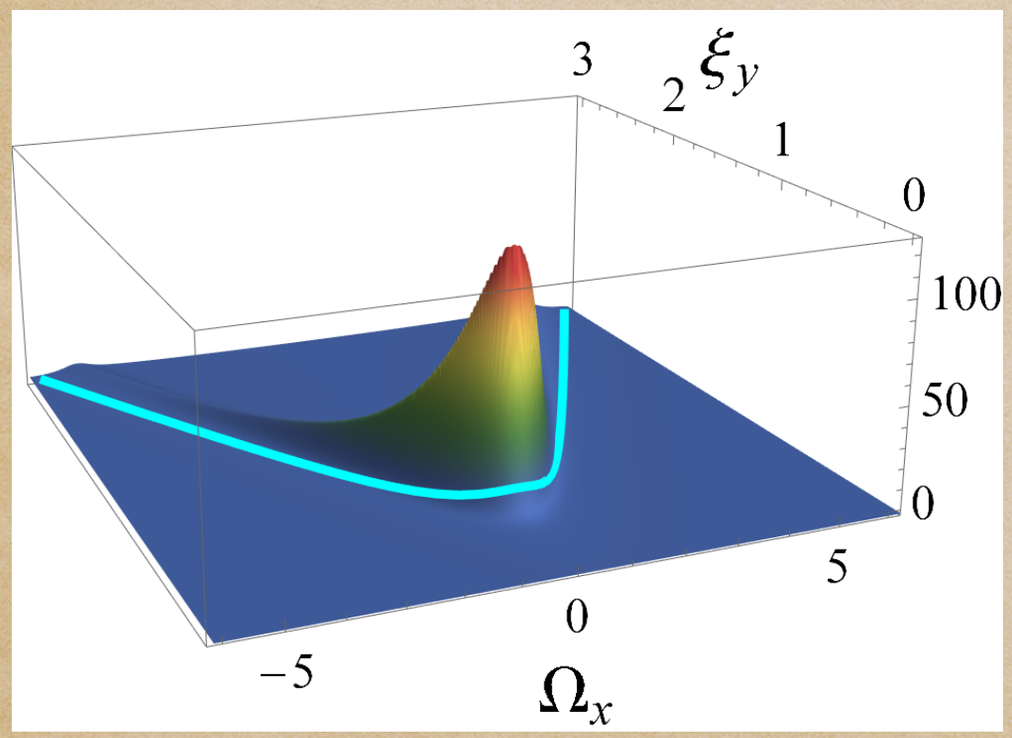
3
2
1
0
ξ_y
100
50
0
5
0
−5
Ω_x

g_{22}

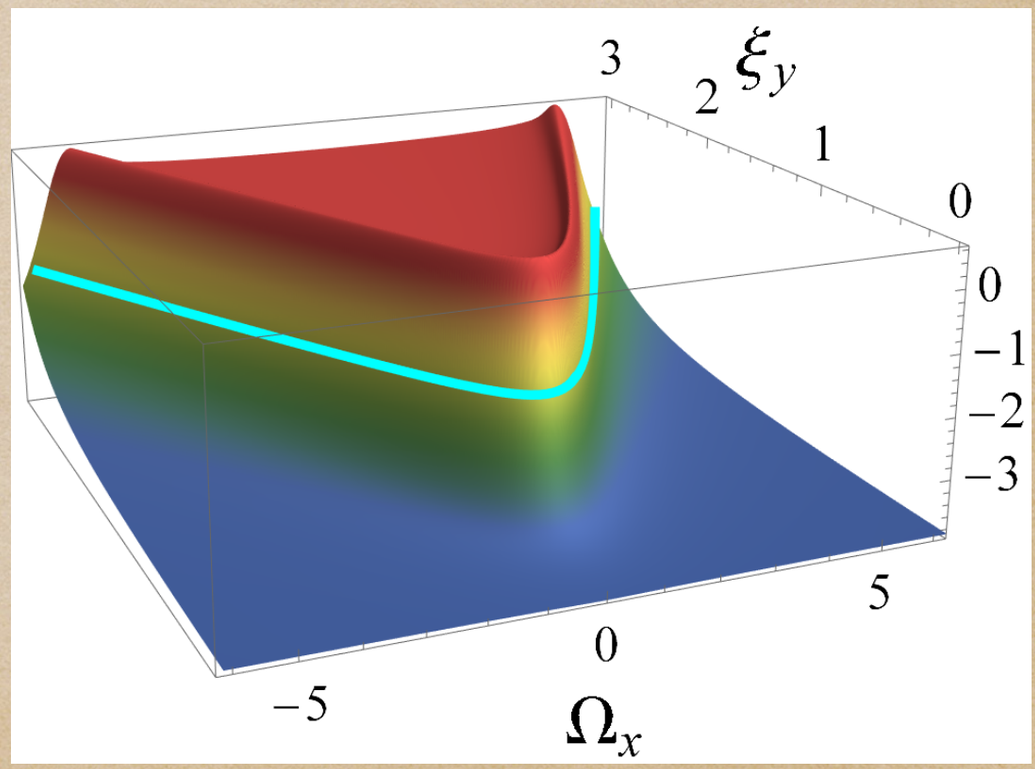
3
2
1
0
ξ_y
0
−1
−2
−3
5
0
−5
Ω_x

R

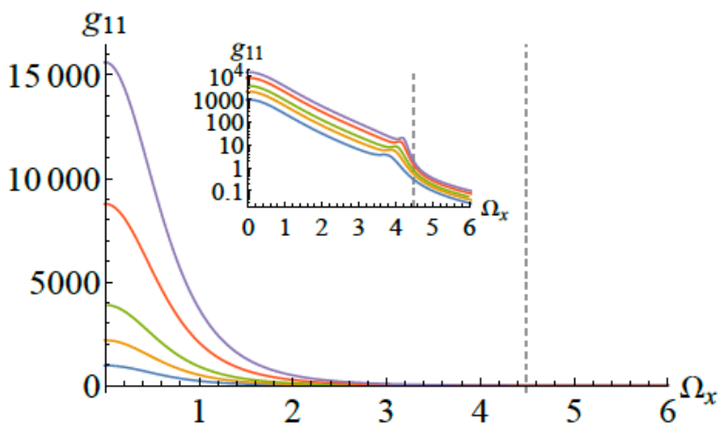

(a) g_{11}

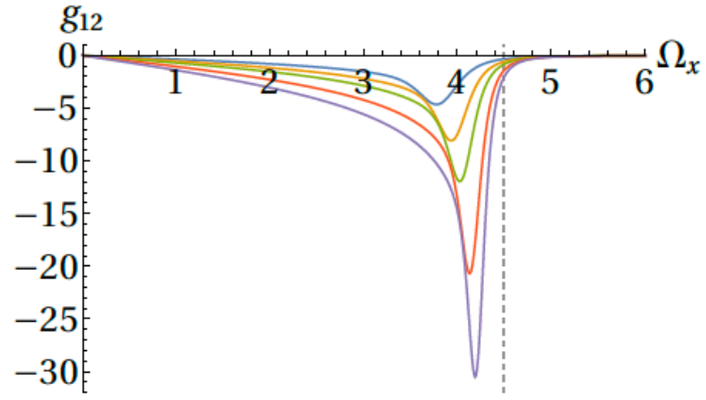

(b) g_{12}

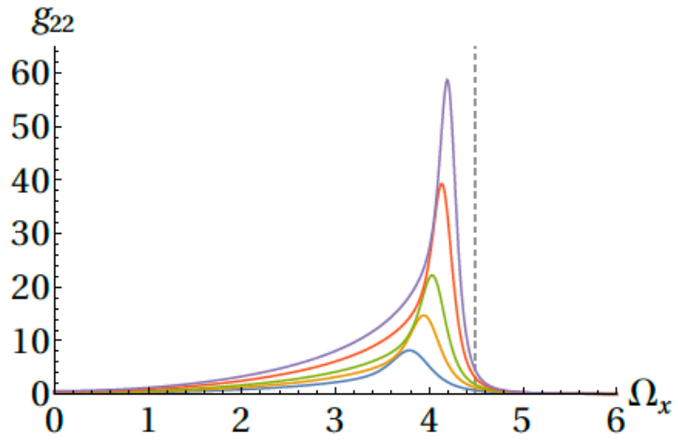

(c) g_{22}

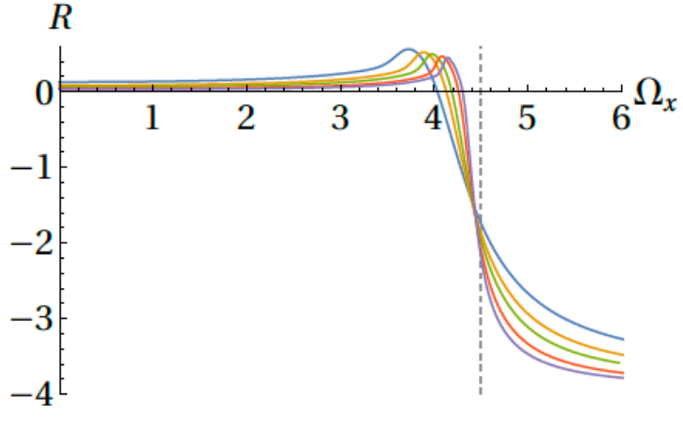

(d) R

FIG. 12. QMT components and scalar curvature for $\xi_y = 2.3$ and $j = 32, 48, 64, 96, 128$. The inset shows the g_{11} component in logarithmic scale.

C. Peaks analysis

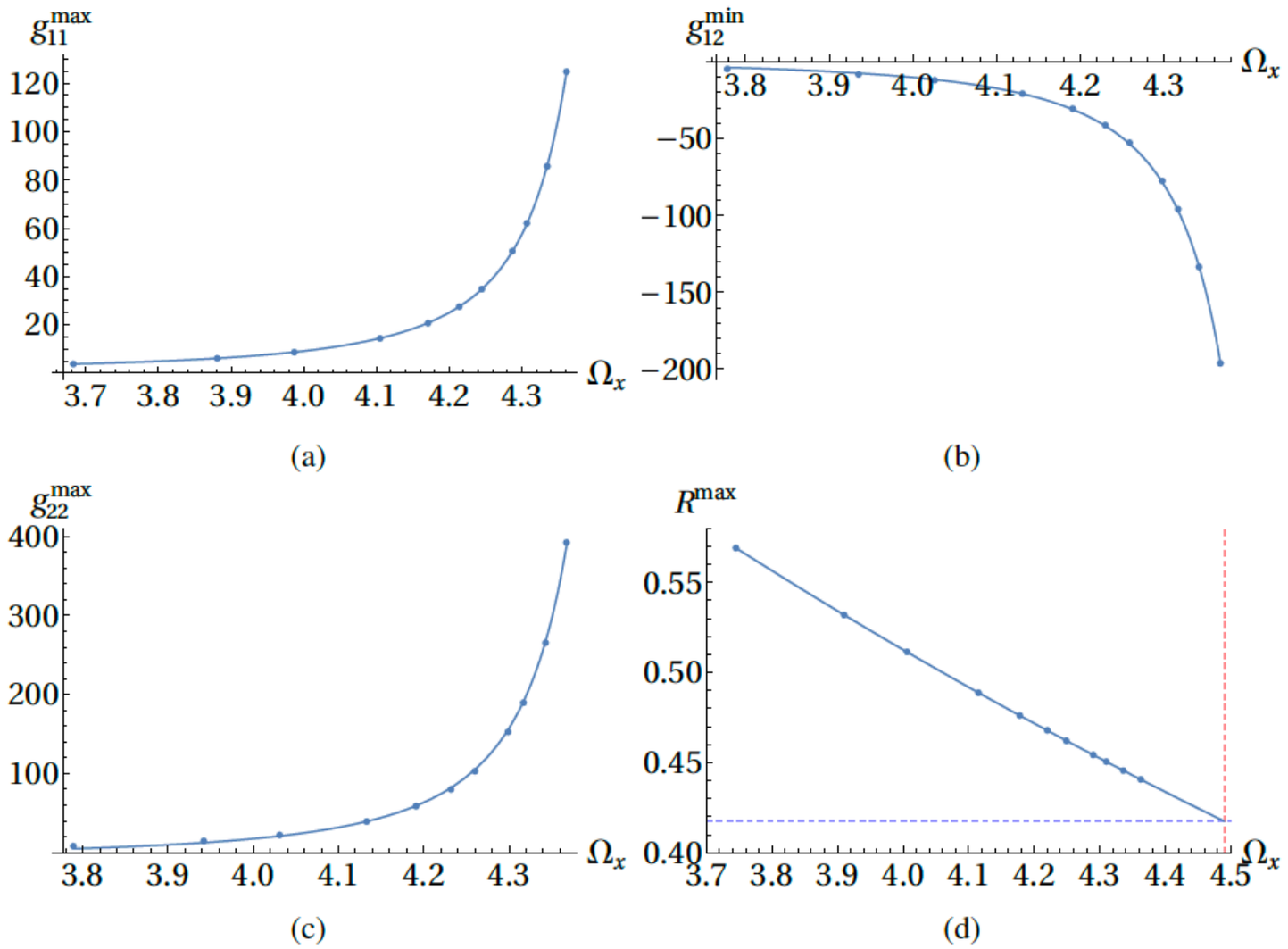

FIG. 13. Behavior of the maximum of each metric component and scalar curvature with respect to Ω_x for $\xi_y = 2.3$. The points correspond to $j = 32, 48, 64, 96, 128, 160, 192, 256, 300, 384, 512$.

Conclusions

- In the Dicke model, we considered the thermodynamic limit under the truncated Holstein-Primakoff approximation and showed that the classical metric and its scalar curvature have similar behavior as their quantum counterparts near the QPT. For the first time, the classical metric was obtained in this case, and the QMT was corroborated under our time-dependent deformation functions approach.

- The resonance condition was analyzed, and a divergence in the scalar curvature was found, as opposed to the non-resonant case; here, too, both the classical and quantum scalars diverge in the same manner.

- In the LMG model, our analysis consisted of two main parts. First, we calculated the classical metric and the QMT in the thermodynamic limit and showed that they are identical, modulo a quantization rule for action variables. Second, we computed the QMT for finite j and compared it with the analytic counterpart, resulting in a remarkable agreement except near the QPT, where the truncated Holstein-Primakoff transformation is not valid anymore.

- We modify the LMG model that we chose has a non-degenerate metric across the parameter space, as opposed to that considered in the previous example, this model allowed us to compute the scalar curvature in both phases. Two critical points were of relevance in our work: the ground state and the highest energy state. The first state did not show any singular behavior in the parameter space under consideration $\xi_y > 0$. On the other hand, the second state exhibited a QPT, and as a result, the QMT components turned out singular. However, in terms of the scalar curvature, the second-order QPT is indicated only as a sudden change of sign and not a singularity. Implying that the singularity appearing in the QMT is removable and is not a true singularity of the parameter space.